

COLOR-INCLINATION RELATION OF THE CLASSICAL KUIPER BELT OBJECTS

NUNO PEIXINHO^{1,2,3}, PEDRO LACERDA¹, AND DAVID JEWITT¹

¹ Institute for Astronomy, University of Hawaii,
2680 Woodlawn Drive, Honolulu, HI 96822, U.S.A.

² Centre for Computational Physics, University of Coimbra, P-3004-516 Coimbra, Portugal and

³ Astronomical Observatory of the University of Coimbra, P-3040-004 Coimbra, Portugal

Accepted for publication in The Astronomical Journal (2008 August 21)

ABSTRACT

We re-examine the correlation between the colors and the inclinations of the Classical Kuiper Belt Objects (CKBOs) with an enlarged sample of optical measurements. The correlation is strong ($\rho = -0.7$) and highly significant ($> 8\sigma$) in the range $0^\circ - 34^\circ$. Nonetheless, the optical colors are independent of inclination below $\approx 12^\circ$, showing no evidence for a break at the reported boundary between the so-called dynamically “hot” and “cold” populations near $\approx 5^\circ$. The commonly accepted parity between the dynamically cold CKBOs and the red CKBOs is observationally unsubstantiated, since the group of red CKBOs extends to higher inclinations. Our data suggest, however, the existence of a different color break. We find that the functional form of the color-inclination relation is most satisfactorily described by a non-linear and stepwise behavior with a color break at $\approx 12^\circ$. Objects with inclinations $\geq 12^\circ$ show bluish colors which are either weakly correlated with inclination or are simply homogeneously blue, whereas objects with inclinations $< 12^\circ$ are homogeneously red.

Subject headings: Kuiper Belt – methods: data analysis – solar system: general

1. INTRODUCTION

The Kuiper Belt is a disk of icy bodies having semi-major axes larger than that of Neptune. Its members are usually known as Kuiper Belt Objects (KBOs) or Trans-Neptunian Objects (TNOs). The distribution of their orbits is structured leading to the identification of several dynamical families. Resonant KBOs are those which are trapped in mean-motion resonances with Neptune (those trapped in the 3:2 resonance are also known as Plutinos). Scattered KBOs, also known as Scattered Disk Objects, are essentially highly eccentric KBOs under strong gravitational influence of Neptune. Classical KBOs (CKBOs) possess relatively circular orbits that are neither located in any strong mean-motion resonance with Neptune nor strongly subject to its gravitational influence.

Since their discovery in 1992 more than 1200 KBOs have been identified. Due to their faintness only about 50 can be spectroscopically studied with the currently available instruments. Multicolor photometry provides, however, a first-order approximation of their spectra, hence of their surface composition. Most KBOs can be studied photometrically and about 230 objects have at least one measured color. Their surface colors have shown to be most diverse, ranging from neutral and even slightly blue (relative to the Sun) to extremely red, suggesting a large compositional diversity (see review by Doressoundiram et al. 2008).

The origin of the color diversity remains unclear. Various suggestions have been made in the context of collisional resurfacing (Luu & Jewitt 1996; Gil-Hutton 2002; Delsanti et al. 2004). Nevertheless, none of the proposed models has been able to consistently explain the colors (Jewitt & Luu 2001; Thébault & Doressoundiram 2003; Delsanti et al. 2004). Another possibility is that the observed color differences reflect primordial compositional

variations (e.g. Tegler et al. 2003). Such compositional differences would be hard to explain if KBOs formed *in situ*, since the temperature difference between 30 and 50 AU is a very modest ≈ 10 K. However, larger temperature and compositional differences might be possible if the KBO population, or part of it, did not form in place. Some dynamical models, in fact, suggest outward migration of KBOs (e.g. Malhotra 1995; Gomes 2003). Although there are no detailed chemical studies to address how varied such compositions would be and how these would reflect in the surface colors, these dynamical models imply a link between the current orbital inclinations of classical KBOs and their presumed location of origin.

As a whole, KBOs do not show significant correlations between their colors and orbital parameters such as semi-major axis or perihelion distance. On the other hand, the CKBOs do show a correlation between orbital inclination and optical color (Tegler & Romanishin 2000; Trujillo & Brown 2002) and a correlation between perihelion and color (Tegler & Romanishin 2000; Peixinho et al. 2004). In parallel, several works have pointed out the existence of two groups of CKBOs with a separation at $\approx 5^\circ$ in inclination. The two groups, usually referred to as “cold” ($i \lesssim 5^\circ$) and “hot” ($i \gtrsim 5^\circ$), have been identified using not only orbital properties (Brown 2001; Elliot et al. 2005) but also physical properties such as size and binarity (Levison & Stern 2001; Peixinho et al. 2004; Gulbis et al. 2006; Noll et al. 2008). Given its potential importance, we re-examine the color-inclination relation using a new data set and appropriate statistical tests.

2. DATA SET

We use the system of Lykawka & Mukai (2007) to select CKBOs for our sample. These authors classify the KBO families based on 4 Gyr dynamical simulations. The Classical KBOs have semi-major axes in the range $37 < a < 48$ AU and perihelion distances $q > 37$ AU,

and must not be located in any strong resonance (3:2, 5:3, 7:4, and 2:1). All orbital elements were gathered from the Minor Planet Center¹. We have computed the orbital inclinations relative to the Kuiper Belt Plane (KBP), hereafter denoted by i_k , as defined by Elliot et al. (2005). We conducted our statistical tests using both the raw inclinations and i_k , finding no significant difference between them. In the remainder of this work, we present all results in terms of i_k .

For our data set we have gathered all the $B - R$ colors of CKBOs available in the literature or online. Several objects have colors reported in more than one work but the different measurements have been shown to be essentially compatible. Hence we chose to take the CKBO colors sequentially from the works that have been presenting lower and less dispersed error bars to those with (slightly) larger and more dispersed error bars. Therefore, firstly we gathered the CKBO colors from Tegler, Romanishin and Consolmagno’s data sample² (Tegler et al. 2003, and references therein); secondly those from the “ESO Large Program on Centaurs and TNOs” (Peixinho et al. 2004, and references therein); thirdly those from the “Meudon Multicolor Survey (2MS)” (Doresoundiram et al. 2005, and references therein); fourthly those from Jewitt et al. (2007); and lastly those from the online Hainaut & Delsanti (2002) MBOSS database³. The resulting CKBO sample used here has colors in the range $0.99 \leq B - R \leq 1.94$. For reference, the color of the Sun is $(B - R)_\odot = 0.99$ (Hartmann et al. 1990).

A histogram of the $B - R$ error bars of the gathered CKBOs shows a rather continuous but very skewed distribution, from 0.01 up to 0.21 peaking around 0.06 and with a mean value of 0.09. Six wayward objects possess errors between 0.28 and 0.40, though, and we chose to eliminate them. The subsequent data consist of the $B - R$ colors of 71 CKBOs (see Table 1). As discussed in the next section, two data points appear to be outliers: 2001QY₂₉₇ and 1998WV₂₄. We chose to discard both and the final data set under analysis consists of the $B - R$ colors of 69 CKBOs. The effects of keeping these two wayward objects in the sample are discussed in Section 3.6.

3. DATA ANALYSIS

A visual inspection of the $B - R$ colors of CKBOs versus i_k in our data set instantly shows a trend between these two variables (see Fig. 1). Using the statistical tools implemented in IDL we have analyzed this trend quantitatively. The Spearman-rank correlation coefficient, ρ , for the total of $N=69$ CKBOs (Spearman 1904) is:

$$\rho = -0.70_{-0.07}^{+0.09} \quad SL > 8\sigma \quad (1)$$

where SL is the significance level in standard deviations of a Gaussian probability distribution — error bars are estimated from 1000 bootstrap extractions corrected for non-Gaussian behavior (Efron & Tibshirani 1993). This is a highly significant correlation consistent with the published values. The square of the correlation coefficient, usually called the “coefficient of determination”, gives

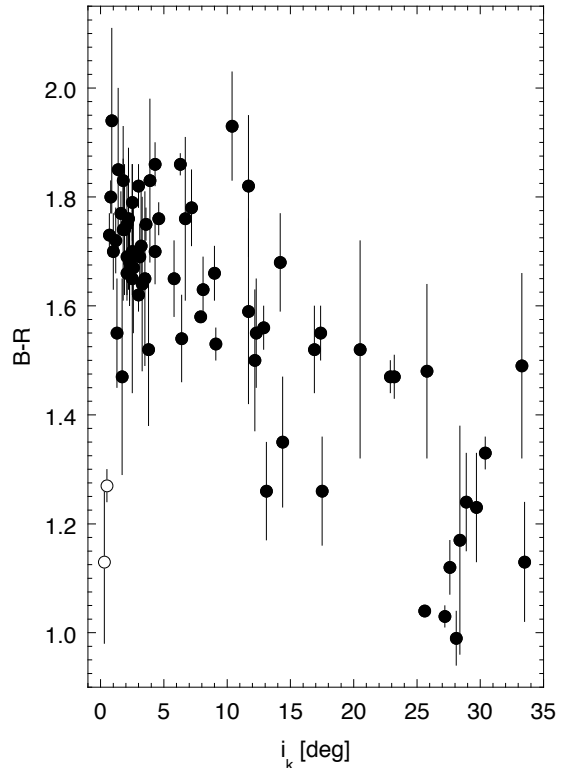


FIG. 1.— $B - R$ colors versus inclination to the Kuiper Belt Plane, i_k [deg], of our data set of 69 CKBOs (black dots). The two apparent outliers that were discarded from our analysis are indicated (empty circles).

approximately the proportion of the variation in the dependent variable that can be predicted by the changes in the values of the independent variable. So, from $\rho^2 = (-0.70)^2 = 0.49$ we may say that about half of the color variability can be accounted for by differences in orbital inclination. The other half is color variability unaccounted for by inclination differences and presumably related to some other undetermined variable or effect.

Fig. 1 suggests that the color-inclination trend might be not linear: the colors of low inclination objects do not seem to correlate with inclination. When dividing the data set in two groups in inclination with equal number of objects we have a low inclination group with 34 objects ($i_k < 5^\circ$) and a high inclination group with 35 ($i_k \geq 5^\circ$). While the high inclination group still shows a strong and significant color-inclination correlation: $\rho = -0.81_{-0.04}^{+0.05}$ ($SL > 8\sigma$), the low inclination one does not show any significant correlation: $\rho = -0.13_{-0.20}^{+0.21}$ ($SL = 0.7\sigma$).

In Fig. 2 we have drawn histograms of the $B - R$ colors for the 34 objects with $i_k < 5^\circ$, for the 46 objects with $i_k < 12^\circ$, and for all objects. From this figure it seems that the color distributions for $i_k < 5^\circ$ and $i_k < 12^\circ$ are the same while only for $i_k \geq 12^\circ$ do we start to see a significant number of blue objects. The color differences between two groups of objects may be analyzed using the Wilcoxon Test (Wilcoxon 1945), the non-parametric equivalent of the t-Test, also known as Wilcoxon Rank-Sum Test. The test ranks the full set of colors and assesses for incompatibility by comparing the ranks assigned to the members of each group. Com-

¹ <http://cfa-www.harvard.edu/iau/lists/TNOs.html>

² <http://www.physics.nau.edu/~teglar/research/survey.htm>

³ <http://www.sc.eso.org/~ohainaut/MBOSS/>

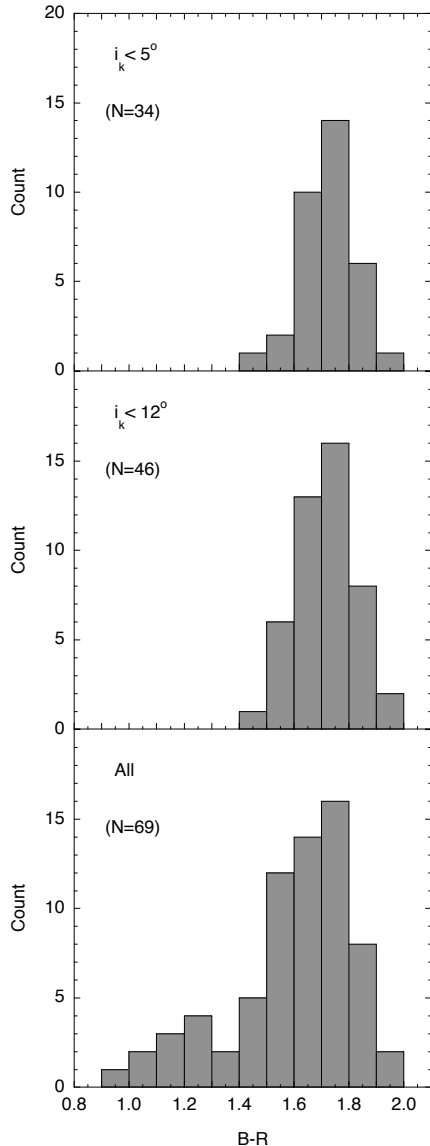


FIG. 2.— Histograms of $B - R$ colors with $i_k < 5^\circ$ (top), with $i_k < 12^\circ$ (middle), and all i_k values (bottom). Only for $i_k \geq 12^\circ$ do we see a significant number of blue objects, whereas objects between 5° and 12° do not appear different from those with $i_k < 5^\circ$.

paring the 34 objects with $i_k < 5^\circ$ and the 12 objects with $5 \leq i_k < 12^\circ$ shows no evidence for color differences between the two groups (the significance level of incompatibility is 0.8σ). On the other hand, comparing the 46 objects with $i_k < 12^\circ$ and the 23 objects with $i_k \geq 12^\circ$ shows a color incompatibility at a 6.3σ significance level. Next we study: (i) how the correlation coefficient varies with the inclusion of more highly inclined objects, (ii) how the mean colors vary with inclination, and (iii) which functional form best describes their behavior.

3.1. Correlation as a function of inclination

To further investigate the variations of the color-inclination trend we have successively computed ρ for CKBOs below a critical inclination cutoff i_k^c varying from 3° in increments of 0.5° up to 20° . These two extrema were imposed so as not to calculate correlation values

for very small sub-samples which were already out of the region of interest. Table 2 lists the results for each inclination cutoff i_k^c , both for objects with inclinations below i_k^c and those above i_k^c — error bars and significance levels are also indicated. We see that ρ varies rather erratically until $i_k^c = 12^\circ$, increases systematically with the inclusion of objects above that point, and reaches the 2σ (95%) typical minimum statistical threshold to have “reasonably strong evidence” for correlation at $i_k^c = 13.5^\circ$. Such behavior suggests the presence of a homogenous set of colors below $i_k \approx 12^\circ - 13.5^\circ$ consistent with Fig. 2. While for the 46 CKBOs with $i_k < 12^\circ$ we have no apparent color-inclination correlation ($\rho = -0.15^{+0.18}_{-0.17}$, $SL = 1.0\sigma$), for the 23 objects with $i_k \geq 12^\circ$ a significant correlation is present ($\rho = -0.62^{+0.14}_{-0.11}$, $SL = 3.2\sigma$). We note that after moving the critical inclination cutoff by just 0.5° the 21 CKBOs with $i_k \geq 12.5^\circ$ no longer show the canonical 3σ level correlation ($\rho = -0.55^{+0.18}_{-0.14}$, $SL = 2.6\sigma$), and for the 17 objects with $i_k \geq 14.5^\circ$ the significance level drops below 2σ ($\rho = -0.45^{+0.28}_{-0.21}$). Thus, the data provide no formally significant evidence for correlation among objects with $i_k \geq 14.5^\circ$.

This first analysis shows that the CKBOs of smallest inclination are homogeneous and red, as other works have reported, but that homogeneity extends at least up to $i_k \approx 12^\circ - 13.5^\circ$, not only up to $i_k \approx 5^\circ$. Further, the rapid decrease in the correlation found by removing the objects between 12° and 14° may suggest two separate groups of objects, each one having no color-inclination correlation whatsoever, populating two distinct parts of the Classical Kuiper Belt. We will address this possibility further ahead.

We are aware, though, that when considering objects with $i_k < i_k^c$ and $i_k \geq i_k^c$ separately we are also reducing the inclination spans under analysis, *i.e.*, constraining the range of inclination values. We saw previously that only about half of the color variability can be explained by inclination differences. Consequently, the weakening of correlation values and their significance levels seen when splitting the data set in two inclination groups, could simply be a consequence of using an inclination range too narrow to detect any significant trend. To investigate this possibility we analyze how the mean colors of CKBOs vary with inclination.

3.2. Color differences as a function of inclination

Evidently, if the sample shows a color-inclination trend the mean colors of CKBOs with $i_k < i_k^c$ must be different from those with $i_k \geq i_k^c$. That is, they must be statistically incompatible. If the trend was approximately linear, evidence for color incompatibility would simply vary smoothly with the number of objects above and below i_k^c , as it also depends on that number. However, if there is a homogenous group of colors below some i_k^c value then a maximum of color incompatibility between objects above and below that i_k^c is expected to occur.

Using the Wilcoxon Test, we successively compare the mean colors of CKBOs having $i_k < i_k^c$ with those having $i_k \geq i_k^c$, varying i_k^c from 3° to 20° in increments of 0.5° . Results for each i_k^c are listed in the last column of Table 2 — the W_{SL} value is the significance level in standard deviations of a Gaussian probability distribution. The mean values are also indicated. The significance of these

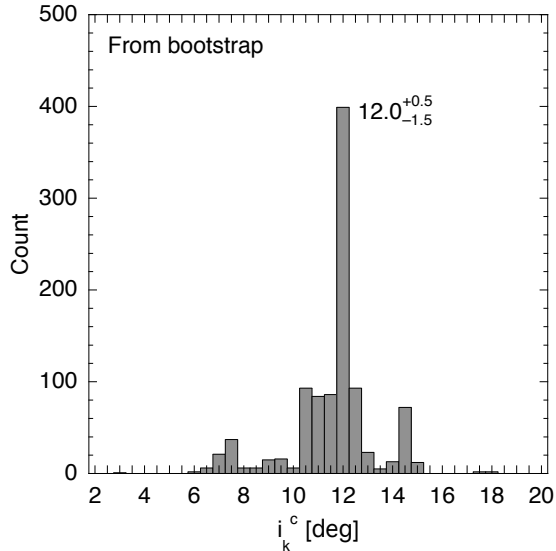


FIG. 3.— Histogram of the probability density distribution of best critical inclination cutoff i_k^c for maximum color differences (from Wilcoxon Tests), obtained by bootstrapping our data sample. The maximum color difference is found at $i_k^c = 12.0^{+0.5}_{-1.5}$.

differences peaks at $i_k^c = 12.0^\circ$, with a value of 6.3σ . These results corroborate the existence of a homogenous set of colors below $i_k \approx 12^\circ$, as suggested by the analysis in the previous sections.

3.3. Confidence intervals for critical inclination cutoff

The finding of the critical inclination cutoff $i_k^c = 12^\circ$ that separates the red group of CKBOs from the more blue ones, carried out in the previous sections, assumes that our data set is a representative sample of the CKBOs. As with the correlation coefficients case, we may use bootstraps to estimate the confidence interval (error bar) of the best inclination cutoff i_k^c obtained from the Wilcoxon Tests. We have made 1000 bootstrap extractions from the data set and for each extraction we have looked for the i_k^c values that maximized the color differences between objects above and below it, as done in the previous section. Since in our analysis the i_k^c is not continuous but discrete (with 0.5° steps) the bootstrap distribution is likely to be jagged. To avoid jaggedness a Gaussian noise with $\sigma = 0.25^\circ$ was added to the inclinations of each bootstrap extraction (smooth bootstrap).

The probability density distribution of best critical inclination cutoff i_k^c for maximum color differences (from Wilcoxon Tests) is shown in Fig. 3. The i_k^c that maximizes color differences is well centered around 12° . Its 1σ confidence interval (68.3% percentile) is $i_k^c = 12.0^{+0.5}_{-1.5}$. The probability density distribution is not smoothly bell-shaped and two other small solution spikes are also present: 5.8% probability for $i_k^c = 7.5^{+0.0}_{-0.5}$ and 9.7% probability at $i_k^c = 14.5^{+0.5}_{-0.5}$. However, the associated probabilities of these spikes are low and they do not warrant further attention.

3.4. The color-inclination relation

Having established that the CKBOs with $i_k \lesssim 12^\circ$ constitute a group of homogeneously red objects, we next examine the variation of $B-R$ at larger inclinations and the

apparent stepwise behavior at the edge of the homogeneously red group. We consider three different functional forms for $B-R$ color as a function of inclination: a) linear; b) two-constant stepwise; c) constant-linear stepwise (see Fig. 4).

3.4.1. Linear fit

Firstly, we performed a simple linear fit to the data, as:

$$(B-R) = m i_k + (B-R)_o \quad (2)$$

where m is the linear slope and $(B-R)_o$ is the intercept. We have used a non-weighted Levenberg-Marquardt least-squares fit (Levenberg 1944; Marquardt 1963). We chose not to weight the data points using their error bars as those refer to the precision of each color measurement and not to the expected departure from the global trend. We have obtained the solution:

$$(B-R) = -0.0182 i_k + 1.774 \quad (3)$$

with a $\chi^2 = 1.208$ and $df = 67$ degrees-of-freedom (see Fig. 4).

3.4.2. Two-constant stepwise fit

Secondly, since our previous analysis also showed the possibility that CKBOs consist of two different homogeneous groups of objects, neither with any color-inclination correlation, we fitted the data with a two-constant stepwise function:

$$\begin{cases} (B-R) = (B-R)_{o1} \Leftarrow i_k < i_k^c \\ (B-R) = (B-R)_{o2} \Leftarrow i_k \geq i_k^c \end{cases} \quad (4)$$

i.e., a stepwise function with a constant color value below a given critical inclination i_k^c , and with another constant value above i_k^c . We have fitted this function to the data iteratively, changing i_k^c from 3° to 20° with increments of 0.5° . For each iteration, $(B-R)_{o1}$ and $(B-R)_{o2}$ are fitted while the critical i_k^c is kept fixed. Table 3 shows the results obtained for each i_k^c value. The best fit, defined as the one which minimizes χ^2 , is obtained when $i_k^c = 13.0^\circ$:

$$\begin{cases} (B-R) = 1.701 \Leftarrow i_k < 13.0^\circ \\ (B-R) = 1.316 \Leftarrow i_k \geq 13.0^\circ \end{cases} \quad (5)$$

with $\chi^2 = 1.349$ and $df = 66$ (see Fig. 4).

3.4.3. Constant-linear stepwise fit

Thirdly, we chose to fit a constant-linear stepwise function:

$$\begin{cases} (B-R) = (B-R)_{o1} \Leftarrow i_k < i_k^c \\ (B-R) = m i_k + (B-R)_{o2} \Leftarrow i_k \geq i_k^c \end{cases} \quad (6)$$

where we have a $(B-R)_{o1}$ constant value below some critical inclination i_k^c , and a linear behavior with slope m and intercept $(B-R)_{o2}$ above i_k^c . As for the previous case, we have fitted this function iteratively changing i_k^c from 3° to 20° with increments of 0.5° . For each iteration $(B-R)_{o1}$, m , and $(B-R)_{o2}$ are fitted while i_k^c is kept fixed. The fitting results for each i_k^c are shown in Table

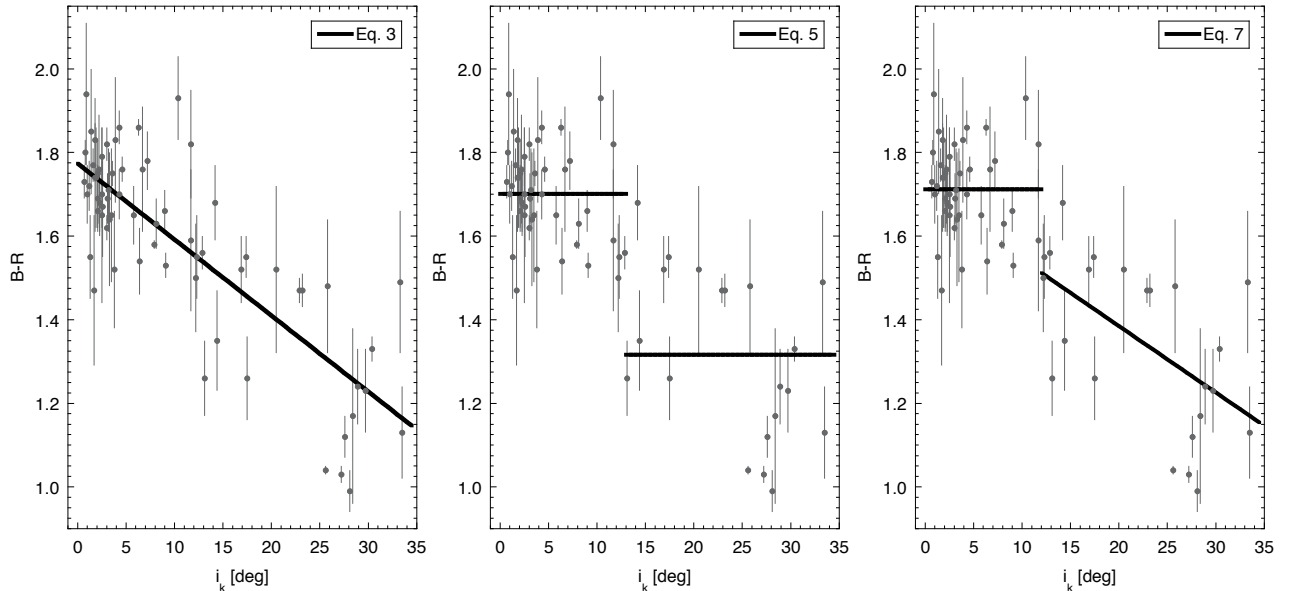


FIG. 4.— Three functional forms studied as possible color-inclination behaviors of CKBOs. Left: Eq. 3 — the linear fit; center: Eq. 5 — the two-constant stepwise fit with $i_k^c = 13^\circ$; right: Eq. 7 — the constant-linear stepwise fit with $i_k^c = 12^\circ$. A χ^2 analysis shows that Eq. 7 is the best fit.

3. The best fit, from the minimum χ^2 , is obtained when $i_k^c = 12.0^\circ$:

$$\begin{cases} (B - R) = 1.712 & \Leftarrow i_k < 12.0^\circ \\ (B - R) = -0.0159 i_k + 1.703 & \Leftarrow i_k \geq 12.0^\circ \end{cases} \quad (7)$$

with $\chi^2 = 1.100$ and $df = 65$ (see Fig. 4). The smallest χ^2 value points to this solution as the best. Note that in our analysis the χ^2 does not tell us the probability of eventually obtaining a better fit if we had another sample of CKBOs (with smaller error bars, for example). This last solution is the best relative to the other cases, and validates our findings as discussed in the previous sections.

3.5. Sharp boundary between groups or overlap?

We have seen that CKBOs up to $i_k = 12^\circ$ are homogeneous in terms of their $B - R$ color (see Fig. 2) and that they are redder than CKBOs with $i_k > 12^\circ$. If this is due to the existence of two independent populations, then we might expect some mixing of the two at inclinations close to the boundary. Such mixing might also be expected from dynamical considerations as cold (low- i_k) CKBOs may be pumped to higher inclinations ($10^\circ \sim 15^\circ$) due to interactions with resonances or even with a potential “planetoid” (*e.g.*, Kuchner et al. 2002; Lykawka & Mukai 2007, 2008).

We cannot compute the χ^2 from the superposition of two functions for direct comparison with the fits obtained in the previous section. However, we have used the functional core-halo inclination decomposition proposed by Elliot et al. (2005) to consider the possibility that the observed color systematics (Fig. 1) result from the overlap of a red core population (low inclinations) with a blue halo population (high inclinations). Simulations show that this solution fails in the sense that it cannot reproduce the color jump observed at 12° . The combination

of the broad inclination distribution for the halo objects (see Fig. 20 of Elliot et al. 2005) and the large color dispersion we observe for the bluer objects ($1\sigma = 0.20$; see also Fig. 2) results in a very smooth and broad color distribution at all inclinations, except for $i_k < 3^\circ$ where red objects are slightly more abundant.

Interestingly, the distribution of $B - R$ colors of CKBOs below $i_k = 12^\circ$ is remarkably Gaussian, which attests to their color homogeneity. The Kolmogorov-Smirnov Test (hereafter KS; Kolmogorov 1933; Smirnov 1939) gives a confidence level of 99.3% (2.7σ) that the colors of $i_k < 12^\circ$ CKBOs are drawn from a Gaussian distribution with mean $\mu = 1.71$ and standard deviation $\sigma = 0.11$ (values calculated from the sample). This stands in contrast to the color distribution of objects above $i_k = 12^\circ$ (mean $\mu = 1.34$ and standard deviation $\sigma = 0.20$) for which the KS Test gives a probability of only 22.5% of being derived from a Gaussian. From the KS Test the whole sample of $B - R$ colors of CKBOs has only a 11.4% probability of being Gaussian.

The lack of a break in the color distribution near 5° stands in sharp contrast to the reportedly bimodal distribution of orbital inclinations (Brown 2001; Elliot et al. 2005). Some models have attempted to relate dynamically cold ($i \lesssim 5^\circ$), red KBOs to a primordial trans-Neptunian disk source while dynamically hotter ($i \gtrsim 5^\circ$), blue KBOs are supposed to originate by outward scattering from sources interior to Neptune (Gomes 2003; Morbidelli et al. 2003). These models make the *ad hoc* assumption that hot and cold KBO populations have intrinsically different colors (blue and red, respectively). This assumption is inconsistent with the data. The $B - R$ distribution pays no regard to the reported hot/cold inclination distribution.

3.6. Double-checks

Some of our objects possess large photometric error bars. Under the penalty of too low sampling we have

also looked for the best fitting solution using only the 48 CKBOs with colors having errors ≤ 0.10 . The best fitting solutions are found with equal probability for Eq. 7 when i_k^c varies from 10.5° to 12.0° (with this sample we have no colors between these two inclination values). When comparing the mean colors of objects above and below i_k^c with this reduced sample we also find equal incompatibility levels for $i_k^c = 10.5^\circ$ up to 12.0° , as expected from the previous result. Also, when not discarding the two apparent outliers mentioned in Section 2 the correlation values diminish slightly but all other results remain identical.

Our sample of CKBOs was selected following a criterion based on the magnitude of the error bars instead of performing an average of all the published measurements for each object as used in the MBOSS sample (see Section 2). To check the influence of this criterion we have double-checked our results using the CKBO colors from the MBOSS sample, since some color values were slightly different from those we have used. The outcome is identical to that of Section 3.4.

Lastly, Gladman et al. (2008) suggest an orbit classification scheme slightly different from the one used here (by Lykawka & Mukai 2007). The classifications of most KBOs remain unchanged between these two schemes and, not surprisingly, we find that our conclusions are statistically independent of the scheme employed.

4. CONCLUSIONS

The main goal of this work has been to investigate the color-inclination trend seen for Classical Kuiper Belt Objects (CKBOs). We have analyzed a sample of $B - R$ colors of 69 objects, excluding 2 apparent outliers as well as colors with error bars larger than 0.21. Objects were classified as CKBOs according to a definition by Lykawka & Mukai (2007). Orbital inclinations, denoted i_k , were calculated relative to the Kuiper Belt Plane following Elliot et al. (2005). Our results may be summarized as:

1. The linear $B - R$ color-inclination correlation of CKBOs measured over the full range of inclinations from 0° to 34° is $\rho = -0.70_{-0.07}^{+0.09}$, corresponding to a significance level larger than 8σ . This is a strong and highly significant correlation, consistent with previously published values.
2. In contrast, the $B - R$ colors of CKBOs with inclinations $i_k \leq 12.0_{-1.5}^{+0.5}$ are statistically uncorrelated with inclination and are well described by $B - R = 1.71 \pm 0.11$.
3. CKBOs with $i_k > 12.0_{-1.5}^{+0.5}$ show a slight color vs. inclination dependence following $(B - R) = -0.0159 i_k + 1.703$. The data are also formally consistent with a constant but bluer color, $B - R = 1.33 \pm 0.20$, for $i_k \geq 12.5^\circ$, and a constant red color $B - R = 1.70 \pm 0.11$ for $i_k < 12.5^\circ$.
4. The data provide no evidence for a break or change in the $B - R$ color distribution at the boundary between the dynamically hot and cold populations, purportedly near $i_k \approx 5^\circ$. In this sense, we find no observational support for the frequently-cited parity between red CKBOs and the dynamically cold population. The CKBOs are red up to $i_k \approx 12^\circ$ and, therefore equally red into the dynamically hot population.

We thank Chadwick Trujillo, Bin Yang, and Rachel Stevenson for comments. NP acknowledges funding from the European Social Fund and the Portuguese Foundation for Science and Technology (FCT, ref.: BPD/18729/2004). PL and DJ benefitted from a grant to DJ from the Planetary Astronomy program of the National Science Foundation.

REFERENCES

- Barucci, M. A., Fulchignoni, M., Birlan, M., Doressoundiram, A., Romon, J., & Boehnhardt, H. 2001, *Astron. Astrophys.*, 371, 1150
- Boehnhardt, H., et al. 2002, *Astron. Astrophys.*, 395, 297
- . 2001, *Astron. Astrophys.*, 378, 653
- Brown, M. E. 2001, *Astrophys. J.*, 121, 2804
- Delsanti, A., Hainaut, O., Jourdeuil, E., Meech, K., Boehnhardt, H., & Barrera, L. 2004, *Astron. Astrophys.*, 417, 1145
- Delsanti, A. C., Boehnhardt, H., Barrera, L., Meech, K. J., Sekiguchi, T., & Hainaut, O. R. 2001, *Astron. Astrophys.*, 380, 347
- Doressoundiram, A., Barucci, M., Romon, J., & Veillet, C. 2001, *Icarus*, 154, 277
- Doressoundiram, A., Peixinho, N., de Bergh, C., Fornasier, S., Thébault, P., Barucci, M. A., & Veillet, C. 2002, *Astron. J.*, 124, 2279
- Doressoundiram, A., Peixinho, N., Doucet, C., Mousis, O., Barucci, M. A., Petit, J. M., & Veillet, C. 2005, *Icarus*, 174, 90
- Doressoundiram, A., Boehnhardt, H., Tegler, S. C., & Trujillo, C. 2008, *The Solar System Beyond Neptune*, 91
- Efron, B., & Tibshirani, R. J. 1993, *An Introduction to the Bootstrap* (Chapman & Hall/CRC)
- Elliot, J. L., et al. 2005, *Astron. J.*, 129, 1117
- Gil-Hutton, R. 2002, *Planet. Space Sci.*, 50, 57
- Gladman, B., Marsden, B. G., & Vanlaerhoven, C. 2008, *The Solar System Beyond Neptune*, 43
- Gomes, R. S. 2003, *Icarus*, 161, 404
- Green, S. F., McBride, N., O Ceallaigh, D. P., Fitzsimmons, A., Williams, I. P., & Irwin, M. J. 1997, *Mon. Not. R. Astron. Soc.*, 290, 186
- Gulbis, A. A. S., Elliot, J. L., & Kane, J. F. 2006, *Icarus*, 183, 168
- Hainaut, O. R., & Delsanti, A. C. 2002, *Astron. Astrophys.*, 389, 641
- Hartmann, W. K., Tholen, D. J., Meech, K. J., & Cruikshank, D. P. 1990, *Icarus*, 83, 1
- Jewitt, D., Peixinho, N., & Hsieh, H. H. 2007, *Astron. J.*, 134, 2046
- Jewitt, D. C., & Luu, J. X. 2001, *Astron. J.*, 122, 2099
- Kolmogorov, A. N. 1933, *Giornale dell' Istituto Italiano degli Attuari*, 4, 83
- Kuchner, M., Brown, M., & Holman, M. 2002, *Astron. J.*, 124, 1221
- Levenberg, K. 1944, *Quart. Appl. Math.*
- Levison, H. F., & Stern, S. A. 2001, *Astrophys. J.*, 121, 1730
- Luu, J., & Jewitt, D. 1996, *Astron. J.*, 112, 2310
- Lykawka, P. S., & Mukai, T. 2008, *Astron. J.*, 135, 116.
- . 2007, *Icarus*, 189, 213
- Malhotra, R. 1995, *Astrophys. J.*, 110, 420
- Marquardt, D. 1963, *SIAM J. Appl. Math.*, 11, 431.
- McBride, N., Green, S. F., Davies, J. K., Tholen, D. J., Sheppard, S. S., Whiteley, R. J., & Hillier, J. K. 2003, *Icarus*, 161, 501
- Morbidelli, A., Brown, M. E., & Levison, H. F. 2003, *Earth Moon and Planets*, 92, 1
- Noll, K. S., Grundy, W. M., Stephens, D. C., Levison, H. F., & Kern, S. D. 2008, *Icarus*

- Peixinho, N., Boehnhardt, H., Belskaya, I., Doressoundiram, A.,
Barucci, M., & Delsanti, A. 2004, *Icarus*, 170, 153
- Romanishin, W., & Tegler, S. C. 1999, *Nature*, 398, 129
- Smirnov, N. V. 1939, *Bull. Moscow Univ.*, 2, 3
- Spearman, C. 1904, *Am. J. Psychol.*, 57, 72
- Tegler, S., & Romanishin, W. 2000, *Nature*, 407, 979
- . 1998, *Nature*, 392, 49
- Tegler, S. C., Romanishin, W., & Consolmagno, S. J. 2003,
Astrophys. J., Lett., 599, L49
- Thébaud, P., & Doressoundiram, A. 2003, *Icarus*, 162, 27
- Trujillo, C. A., & Brown, M. E. 2002, *Astrophys. J., Lett.*, 566,
L125
- Wilcoxon, F. 1945, *Biometrika*, 1, 80

TABLE 1
 DATA SAMPLE

Object	i_k [°] ^a	i [°] ^b	$B - R$	H_R ^c	Ref. ^d	
	2001QY297	0.3	1.5	1.13 ± 0.15	4.97 ± 0.23	Dor+05
	1998WV24	0.5	1.5	1.27 ± 0.03	6.93 ± 0.01	TR00
	1998KS65	0.7	1.2	1.73 ± 0.04	6.99 ± 0.02	TR03
(85633)	1998KR65	0.8	1.2	1.80 ± 0.03	6.43 ± 0.03	TR03
	1999CO153	0.9	0.8	1.94 ± 0.17	6.60 ± 0.03	MB(a)
(15760)	1992QB1	1.0	2.2	1.70 ± 0.07	6.83 ± 0.03	TR00
(134860)	2000OJ67	1.2	1.1	1.72 ± 0.06	5.87 ± 0.07	Dor+02
(52747)	1998HM151	1.3	0.5	1.55 ± 0.10	7.40 ± 0.05	TR03
	2000CL104	1.4	1.2	1.85 ± 0.15	6.87 ± 0.06	Boe+02
	2000FS53	1.6	2.1	1.77 ± 0.04	7.17 ± 0.06	TR03
(66652)	1999RZ253	1.7	0.6	1.47 ± 0.18	5.42 ± 0.06	MB(b)
	1994EV3	1.8	1.7	1.74 ± 0.13	7.53 ± 0.09	Boe+02
(66452)	1999OF4	1.8	2.7	1.83 ± 0.10	6.10 ± 0.09	Pei+04
	1999OM4	1.9	2.1	1.74 ± 0.12	7.43 ± 0.06	Boe+02
(79360)	1997CS29	2.1	2.2	1.69 ± 0.08	4.91 ± 0.11	TR98
(119951)	2002KX14	2.1	0.4	1.66 ± 0.04	4.25 ± 0.03	TRC07
	2003GH55	2.1	1.1	1.75 ± 0.08	5.90 ± 0.05	JPH07
	1998KG62	2.2	0.8	1.76 ± 0.13	6.92 ± 0.08	Boe+02
(19255)	1994VK8	2.3	1.5	1.68 ± 0.07	6.86 ± 0.42	TR00
	1999OJ4	2.3	4.0	1.68 ± 0.08	6.71 ± 0.06	Pei+04
	1994ES2	2.5	1.1	1.65 ± 0.21	7.52 ± 0.12	MB(c)
	1998WX24	2.5	0.9	1.79 ± 0.07	6.09 ± 0.04	TR00
(60454)	2000CH105	2.5	1.2	1.70 ± 0.08	6.20 ± 0.05	Pei+04
(58534) Logos	1997CQ29	2.6	2.9	1.67 ± 0.12	6.70 ± 0.02	Bar+01
	1996TK66	3.0	3.3	1.62 ± 0.03	6.12 ± 0.03	TR00
(24978)	1998HJ151	3.0	2.4	1.82 ± 0.04	6.96 ± 0.02	TR03
(137294)	1999RE215	3.1	1.4	1.69 ± 0.06	6.45 ± 0.17	Boe+02
(33001)	1997CU29	3.2	1.5	1.71 ± 0.10	6.12 ± 0.06	Dor+01
	2001QD298	3.3	5.0	1.64 ± 0.16	4.48 ± 0.08	Dor+05
(148780)	2001UQ18	3.5	5.2	1.65 ± 0.16	5.82 ± 0.21	Dor+05
(16684)	1994JQ1	3.6	3.7	1.75 ± 0.03	6.51 ± 0.03	TR03
	2000CL105	3.8	4.2	1.52 ± 0.14	6.76 ± 0.06	MB(a)
	1999OE4	3.9	2.2	1.83 ± 0.15	6.76 ± 0.17	Pei+04
	1999HS11	4.3	2.6	1.86 ± 0.04	6.16 ± 0.03	TR03
	1999HV11	4.3	3.2	1.70 ± 0.06	6.88 ± 0.03	TR03
	2000CN105	4.6	3.4	1.76 ± 0.03	5.21 ± 0.05	JPH07
	1999RX214	5.8	4.8	1.65 ± 0.07	6.32 ± 0.05	Pei+04
	1997CV29	6.3	8.0	1.86 ± 0.02	7.06 ± 0.01	TR03
(138537)	2000OK67	6.4	4.9	1.54 ± 0.08	5.92 ± 0.07	Dor+02
	1999GS46	6.7	5.2	1.76 ± 0.15	6.23 ± 0.02	MB(a)
	1996TS66	7.2	7.4	1.78 ± 0.07	5.74 ± 0.08	TR98
(50000) Quaoar	2002LM60	7.9	8.0	1.58 ± 0.01	2.10 ± 0.01	TRC03
(79983)	1999DF9	8.1	9.8	1.63 ± 0.06	5.62 ± 0.07	Dor+02
	1993FW	9.0	7.7	1.66 ± 0.05	6.46 ± 0.01	TR03
	1998FS144	9.1	9.8	1.53 ± 0.03	6.60 ± 0.02	TR03
	1999CB119	10.4	8.7	1.93 ± 0.10	6.57 ± 0.05	Pei+04
	1999JD132	11.7	10.5	1.59 ± 0.17	6.00 ± 0.02	MB(a)
	2001KA77	11.7	11.9	1.82 ± 0.13	4.95 ± 0.04	Pei+04
	2002GJ32	12.2	11.6	1.50 ± 0.13	5.48 ± 0.15	Dor+05
	1997RT5	12.3	12.7	1.55 ± 0.10	7.46 ± 0.07	Boe+02
(19521) Chaos	1998WH24	12.9	12.1	1.56 ± 0.04	4.32 ± 0.01	TR00
	1999RY214	13.1	13.7	1.26 ± 0.09	6.96 ± 0.04	Pei+04
	1997QH4	14.2	13.2	1.68 ± 0.09	6.77 ± 0.04	TR00
	1999CQ133	14.4	13.3	1.35 ± 0.12	6.68 ± 0.05	MB(a)
(20000) Varuna	2000WR106	16.9	17.2	1.52 ± 0.08	3.36 ± 0.05	TR03
	2000KK4	17.4	19.1	1.55 ± 0.05	5.82 ± 0.02	TR03
(15883)	1997CR29	17.5	19.2	1.26 ± 0.10	6.95 ± 0.08	Dor+01
	2000CO105	20.5	19.3	1.52 ± 0.20	5.67 ± 0.18	MB(a)
(55565)	2002AW197	22.9	24.4	1.47 ± 0.03	3.07 ± 0.02	TRC07
(90568)	2004GV9	23.2	21.9	1.47 ± 0.04	3.62 ± 0.03	TRC07
(24835)	1995SM55	25.6	27.1	1.04 ± 0.01	4.15 ± 0.01	TR03
	2002GH32	25.8	26.6	1.48 ± 0.16	6.05 ± 0.28	Dor+05
(55636)	2002TX300	27.2	25.9	1.03 ± 0.02	3.11 ± 0.01	TRC03
(19308)	1996TO66	27.6	27.5	1.12 ± 0.05	4.38 ± 0.05	TR98
	2003UZ117	28.1	27.5	0.99 ± 0.05	4.85 ± 0.05	TRC07
	2000CG105	28.4	28.0	1.17 ± 0.21	6.77 ± 0.16	MB(a)
	2001QC298	28.9	30.6	1.24 ± 0.09	6.39 ± 0.05	JPH07
	1998WT31	29.7	28.7	1.23 ± 0.10	7.40 ± 0.04	Pei+04
(136472)	2005FY9	30.4	29.0	1.33 ± 0.03	-0.38 ± 0.05	JPH07
	1996RQ20	33.3	31.7	1.49 ± 0.17	6.89 ± 0.10	MB(d)
	2002PP149	33.5	34.7	1.13 ± 0.11	7.24 ± 0.05	JPH07

^a Orbital inclination relative to the Kuiper Belt Plane^b Orbital inclination relative to the Ecliptic^c Absolute R -magnitude^d References: TRC07, <http://www.physics.nau.edu/~teglar/research/survey.htm>; TRC03, Tegler et al. (2003); TR00, Tegler & Romanishin (2000); TR98, Tegler & Romanishin (1998); Boe+02, Boehnhardt et al. (2002); Pei+04, Peixinho et al. (2004); JPH07, Jewitt et al. (2007); Dor+05, Doressoundiram et al. (2005); Dor+02, Doressoundiram et al. (2002); Dor+01, Doressoundiram et al. (2001); Bar+01, Barucci et al. (2001); MB, MBOSS compilation (Hainaut & Delsanti 2002) – (a) Trujillo & Brown (2002) – (b) Delsanti et al. (2001); Doressoundiram et al. (2001); McBride et al. (2003) – (c) Green et al. (1997); Luu & Jewitt (1996) – (d) Tegler & Romanishin (1998); Romanishin & Tegler (1999); Boehnhardt et al. (2001); Delsanti et al. (2001); Jewitt & Luu (2001)

TABLE 2
CORRELATIONS AND WILCOXON TESTS FOR CONSECUTIVE INCLINATION CUTOFFS

$i_k^c [^\circ]^a$	Objects w/ $i_k < i_k^c$				Objects w/ $i_k \geq i_k^c$				W_{SL}^f
	N_l^b	μ_l^c	$\rho_{l-\sigma}^{+\sigma d}$	SL_l^e	N_h^b	μ_h^c	$\rho_{h-\sigma}^{+\sigma d}$	SL_h^e	
3.0	22	1.721	$-0.34_{-0.18}^{+0.21}$	1.6	47	1.528	$-0.79_{-0.04}^{+0.06}$	> 8	3.5
3.5	27	1.717	$-0.35_{-0.18}^{+0.21}$	1.8	42	1.508	$-0.81_{-0.04}^{+0.05}$	> 8	3.8
4.0	31	1.713	$-0.28_{-0.19}^{+0.21}$	1.5	38	1.489	$-0.84_{-0.04}^{+0.04}$	> 8	4.1
4.5	33	1.717	$-0.17_{-0.19}^{+0.20}$	1.0	36	1.473	$-0.82_{-0.04}^{+0.05}$	> 8	4.6
5.0	34	1.718	$-0.13_{-0.20}^{+0.19}$	0.7	35	1.465	$-0.81_{-0.04}^{+0.05}$	> 8	4.8
5.5	34	1.718	$-0.13_{-0.18}^{+0.19}$	0.7	35	1.465	$-0.81_{-0.04}^{+0.05}$	> 8	4.8
6.0	35	1.716	$-0.17_{-0.18}^{+0.20}$	1.0	34	1.459	$-0.81_{-0.04}^{+0.05}$	> 8	4.8
6.5	37	1.715	$-0.15_{-0.20}^{+0.21}$	0.9	32	1.444	$-0.81_{-0.05}^{+0.06}$	> 8	5.0
7.0	38	1.717	$-0.11_{-0.19}^{+0.19}$	0.7	31	1.434	$-0.80_{-0.05}^{+0.06}$	5.4	5.3
7.5	39	1.718	$-0.07_{-0.18}^{+0.19}$	0.4	30	1.423	$-0.78_{-0.05}^{+0.07}$	5.2	5.6
8.0	40	1.715	$-0.12_{-0.18}^{+0.19}$	0.7	29	1.417	$-0.78_{-0.06}^{+0.07}$	5.0	5.5
8.5	41	1.713	$-0.17_{-0.17}^{+0.18}$	1.0	28	1.410	$-0.76_{-0.07}^{+0.09}$	4.7	5.5
9.0	41	1.713	$-0.17_{-0.16}^{+0.17}$	1.0	28	1.410	$-0.76_{-0.06}^{+0.08}$	4.7	5.5
9.5	43	1.707	$-0.24_{-0.15}^{+0.16}$	1.6	26	1.395	$-0.74_{-0.09}^{+0.12}$	4.3	5.4
10.0	43	1.707	$-0.24_{-0.17}^{+0.18}$	1.6	26	1.395	$-0.74_{-0.09}^{+0.12}$	4.3	5.4
10.5	44	1.712	$-0.17_{-0.17}^{+0.18}$	1.1	25	1.374	$-0.70_{-0.09}^{+0.12}$	3.9	5.9
11.0	44	1.712	$-0.17_{-0.17}^{+0.18}$	1.1	25	1.374	$-0.70_{-0.09}^{+0.12}$	3.9	5.9
11.5	44	1.712	$-0.17_{-0.17}^{+0.18}$	1.1	25	1.374	$-0.70_{-0.09}^{+0.12}$	3.9	5.9
12.0	46	1.712	$-0.15_{-0.17}^{+0.18}$	1.0	23	1.345	$-0.62_{-0.11}^{+0.14}$	3.2	6.3
12.5	48	1.704	$-0.24_{-0.16}^{+0.17}$	1.6	21	1.328	$-0.55_{-0.14}^{+0.18}$	2.6	6.1
13.0	49	1.701	$-0.27_{-0.15}^{+0.17}$	1.9	20	1.317	$-0.48_{-0.15}^{+0.18}$	2.2	6.0
13.5	50	1.692	$-0.32_{-0.15}^{+0.17}$	2.2	19	1.319	$-0.54_{-0.17}^{+0.23}$	2.4	5.8
14.0	50	1.692	$-0.32_{-0.15}^{+0.17}$	2.2	19	1.319	$-0.54_{-0.16}^{+0.22}$	2.4	5.8
14.5	52	1.686	$-0.36_{-0.14}^{+0.15}$	2.6	17	1.296	$-0.45_{-0.21}^{+0.28}$	1.8	5.7
15.0	52	1.686	$-0.36_{-0.14}^{+0.15}$	2.6	17	1.296	$-0.45_{-0.21}^{+0.27}$	1.8	5.7
15.5	52	1.686	$-0.36_{-0.14}^{+0.15}$	2.6	17	1.296	$-0.45_{-0.20}^{+0.26}$	1.8	5.7
16.0	52	1.686	$-0.36_{-0.14}^{+0.15}$	2.6	17	1.296	$-0.45_{-0.21}^{+0.27}$	1.8	5.7
16.5	52	1.686	$-0.36_{-0.14}^{+0.15}$	2.6	17	1.296	$-0.45_{-0.20}^{+0.26}$	1.8	5.7
17.0	53	1.682	$-0.39_{-0.13}^{+0.15}$	2.9	16	1.282	$-0.35_{-0.24}^{+0.29}$	1.3	5.7
17.5	54	1.680	$-0.41_{-0.12}^{+0.14}$	3.0	15	1.265	$-0.21_{-0.28}^{+0.32}$	0.8	5.6
18.0	55	1.672	$-0.44_{-0.12}^{+0.14}$	3.4	14	1.265	$-0.19_{-0.32}^{+0.37}$	0.7	5.4
18.5	55	1.672	$-0.44_{-0.12}^{+0.15}$	3.4	14	1.265	$-0.19_{-0.31}^{+0.35}$	0.7	5.4
19.0	55	1.672	$-0.44_{-0.13}^{+0.15}$	3.4	14	1.265	$-0.19_{-0.32}^{+0.36}$	0.7	5.4
19.5	55	1.672	$-0.44_{-0.12}^{+0.14}$	3.4	14	1.265	$-0.19_{-0.31}^{+0.35}$	0.7	5.4
20.0	55	1.672	$-0.44_{-0.12}^{+0.14}$	3.4	14	1.265	$-0.19_{-0.32}^{+0.37}$	0.7	5.4

^a Orbital inclination cutoff

^b Number of objects below (l) and above (h) the cutoff i_k^c

^c Mean $B - R$ of objects below (l) and above (h) i_k^c

^d $B - R$ vs. i_k correlation for objects below (l) and above (h) i_k^c

^e Significance level of the correlation

^f Significance level of the Wilcoxon Test for color difference between objects below and above i_k^c

TABLE 3
FIT RESULTS FOR CONSECUTIVE INCLINATION CUTOFFS

i_k^c [°] ^a	Two-constant stepwise fit ^b			Constant-linear stepwise fit ^c			
	$(B-R)_{o1}$	$(B-R)_{o2}$	χ^2	$(B-R)_{o1}$	m	$(B-R)_{o2}$	χ^2
3.0	1.721	1.528	2.892	1.721	-0.0194	1.801	1.197
3.5	1.717	1.508	2.737	1.717	-0.0201	1.817	1.188
4.0	1.713	1.489	2.597	1.713	-0.0210	1.837	1.174
4.5	1.717	1.473	2.427	1.717	-0.0207	1.830	1.180
5.0	1.718	1.465	2.344	1.718	-0.0206	1.827	1.181
5.5	1.718	1.465	2.344	1.718	-0.0206	1.827	1.181
6.0	1.716	1.459	2.314	1.716	-0.0208	1.834	1.182
6.5	1.715	1.444	2.191	1.715	-0.0208	1.834	1.183
7.0	1.717	1.434	2.090	1.717	-0.0205	1.825	1.180
7.5	1.718	1.423	1.971	1.718	-0.0198	1.809	1.173
8.0	1.715	1.417	1.964	1.715	-0.0203	1.821	1.185
8.5	1.713	1.410	1.924	1.713	-0.0205	1.825	1.192
9.0	1.713	1.410	1.924	1.713	-0.0205	1.825	1.192
9.5	1.707	1.395	1.876	1.707	-0.0212	1.844	1.213
10.0	1.707	1.395	1.876	1.707	-0.0212	1.844	1.213
10.5	1.712	1.374	1.627	1.712	-0.0187	1.777	1.155
11.0	1.712	1.374	1.627	1.712	-0.0187	1.777	1.155
11.5	1.712	1.374	1.627	1.712	-0.0187	1.777	1.155
12.0	1.712	1.345	1.389	1.712	-0.0159	1.703	1.100
12.5	1.704	1.328	1.385	1.704	-0.0155	1.691	1.166
13.0	1.701	1.316	1.349	1.701	-0.0145	1.665	1.181
13.5	1.692	1.319	1.537	1.692	-0.0182	1.765	1.315
14.0	1.692	1.319	1.537	1.692	-0.0182	1.765	1.315
14.5	1.686	1.296	1.512	1.686	-0.0176	1.748	1.376
15.0	1.686	1.296	1.512	1.686	-0.0176	1.748	1.376
15.5	1.686	1.296	1.512	1.686	-0.0176	1.748	1.376
16.0	1.686	1.296	1.512	1.686	-0.0176	1.748	1.376
16.5	1.686	1.296	1.512	1.686	-0.0176	1.748	1.376
17.0	1.682	1.282	1.486	1.682	-0.0158	1.696	1.397
17.5	1.680	1.265	1.427	1.680	-0.0114	1.570	1.391
18.0	1.672	1.265	1.600	1.672	-0.0175	1.746	1.544
18.5	1.672	1.265	1.600	1.672	-0.0175	1.746	1.544
19.0	1.672	1.265	1.600	1.672	-0.0175	1.746	1.544
19.5	1.672	1.265	1.600	1.672	-0.0175	1.746	1.544
20.0	1.672	1.265	1.600	1.672	-0.0175	1.746	1.544

^a Critical orbital inclination value, *i.e.* location of stepwise behavior.

^b See §3.4.2 and Eq. 4.

^c See §3.4.3 and Eq. 6.